Supporting Information

Nanoscale curvature promotes high yield spontaneous formation of cell-mimetic giant phospholipid vesicles from nanocellulose paper

Joseph Pazzi[§], Anand Bala Subramaniam[§,*]

§ Department of Bioengineering, University of California, Merced, Merced, CA 95343, United States.

Corresponding Author: asubramaniam@ucmerced.edu

1. Supporting Text

Calculations of the change in energy for planar, cylindrical, and spherical substrate geometries

1. Change in energy of a flat membrane disk with radius R_d to a spherical membrane bud with radius R_B

$$E_1 = \pi {R_d}^2 \xi \tag{1.1}$$

$$E_2 = 8\pi\kappa_B + 2\pi R_d \lambda \tag{1.2}$$

$$\Delta E_{R_B,d} = E_2 - E_1 = 8\pi\kappa_B + 2\pi R_d \lambda - \pi {R_d}^2 \xi \tag{1.3}$$

Setting $\Delta E = 0$ and solving for R_d^* gives us:

$$R_d^* = \frac{\lambda + \sqrt{(\lambda^2 + \xi + 8\kappa_B \xi)}}{\xi} \tag{1.4}$$

There are no physical values of R_d where $\Delta E_{R_B,d} \leq 0$ for $\xi \leq 0$, e.g. for attractive or zero adhesion potentials. If there are lipid sources, no breaks in the membrane are required. In this case, $\lambda = 0$.

Area constraint:

$$R_B = \frac{R_d}{2} \tag{1.5}$$

2. Change in energy of a cylindrical membrane section of radius R_c and length L_c to a spherical membrane bud of radius R_B

$$E_1 = \frac{\pi \kappa_B L_c}{R_c} + 2\pi R_c L_c \xi \tag{2.1}$$

$$E_2 = 8\pi\kappa_B + 4\pi R_c \lambda \tag{2.2}$$

$$\Delta E_{R_B,c} = E_2 - E_! = \pi\kappa_B \left(8 - \frac{L_c}{R_c}\right) + 4\pi R_c \lambda - 2\pi R_c L_c \xi \tag{2.3}$$

Setting $\Delta E = 0$ and solving for L_c^* gives:

$$L_c^* = \frac{8\lambda R_c^2 + 8\kappa_B R_c}{\kappa_B + 2\xi R_c^2} \tag{2.4}$$

For attractive interactions, i.e. when ξ is negative, L_c^* is undefined when $\kappa_B = 2\xi R_c^2$ and becomes negative when $|\kappa_B| < |2\xi R_c^2|$ which are unphysical solutions. If there are lipid sources, no breaks in the membrane are required. In this case, $\lambda = 0$.

Area constraint:

$$R_{cyl} L_{cyl} = 2R_B^2 \tag{2.5}$$

3. Change in energy from a hemispherical membrane with radius R_s to a spherical membrane bud of radius R_B

$$E_1 = 4\pi\kappa_B + 2\pi R_s^2 \, \xi \tag{3.1}$$

$$E_2 = 8\pi\kappa_B + 4\pi R_s\lambda \tag{3.2}$$

$$\Delta E_{R_B,S} = 4\pi\kappa_B + 4\pi R_s\lambda - 2\pi R_s^2\xi \tag{3.3}$$

$$R^*_{B,S} = \frac{\lambda - \sqrt{(\lambda^2 + 2\kappa_B\xi)}}{\xi} \tag{3.4}$$

There are no value of $R_s > 0$ where $\Delta E_{R_B,S} < 0$ for $\xi \leq 0$, e.g. for attractive or zero adhesion potentials. If there are lipid sources, no breaks in the membrane are required. In this case, $\lambda = 0$.

Area constraint:

$$R_s^2 = 2R_B^2 \tag{3.5}$$

2. Supporting Methods

1. Cleaning of substrates

Nanocellulose paper and artist grade tracing paper: Out of an abundance of caution, we exhaustively cleaned the paper substrates to remove adventitious soluble hydrophilic and hydrophobic materials. Control experiments using tracing paper as purchased without any cleaning showed no discernible difference in the yields or sizes of GUVs. Working in a chemical fume hood, we soaked the substrates in 100 mL of chloroform in a 500 mL glass beaker while applying occasional manual agitation. We allowed the substrate to soak for 30 minutes and then discarded the chloroform. We repeated the process with fresh chloroform. We removed the substrates from the chloroform and allowed residual solvent to evaporate by leaving the paper in the fume hood for 30 minutes. We then soaked the substrates in ultrapure water. After 30 minutes, we discarded the ultrapure water and repeated the process with fresh ultrapure water. We placed the papers flat in a glass petri dish before placing the dish in a 65 °C oven for 2 hours to dry.

Regenerated Cellulose Dialysis Membranes: We followed the manufacturer's instructions to remove the humectant glycerol and traces of heavy metals and sulfur compounds from the regenerated cellulose dialysis membrane. Briefly, we cut the dry dialysis tubing into 10 cm long pieces and agitate the tubing in 50 mL of ultrapure for 30 minutes. We then cut the tubing open lengthwise and transfer the tubing to new clean glass beaker filled with fresh ultrapure water for a further 60-minute incubation. We next agitate the tubing in a 10 mM solution of sodium bicarbonate at 80°C for 30 minutes. Then we incubated the tubing in a solution of 10 mM EDTA for 30 minutes at room temperature. We finally rinse the tubing under flowing ultrapure water for 10 minutes and transfer the tubing into a clean glass jar with ultrapure water at 80°C while stirring with a magnetic stirrer for 30 minutes. We removed the tubing pieces from the water and wound

the wet membrane around a glass slide and allowed it to dry ambiently. Winding the tubing around a glass slide prevented excessive wrinkling or shrinking of the tubing as it dried.

Glass slides and ITO-covered slides: The electric field degrades ITO-covered slides each time it is used[1]. The degradation results in lower yields of GUVs and results in GUVs of smaller sizes[1]. Annealing in air at 150 °C for 20 minutes is reported to reverse these effects[1]. To ensure the highest possible yields from electroformation while nominally mimicking the pattern of use of this expensive substrate in a typical laboratory, we reuse pristine ITO-covered slides a maximum of five times. Before each use, we cleaned the slides to remove adventitious hydrophobic or hydrophilic materials by sonicating sequentially for 10 minutes in acetone, ethanol, and ultrapure water. We then dried the slides and annealed the slides in air at 150 °C for 20 minutes[1].

2. Hydrophobic modification of the substrates

Silanization of glass slides: We performed vapor phase silanization of plasma-cleaned glass slides using methyltrichlorosilane following previously reported protocols[2]. We placed 0.5 mL of neat methyltrichlorosilane in a 10 mL glass vial. Working quickly to minimize exposure to atmospheric moisture, we placed the uncapped glass vial containing the silane in a laboratory vacuum chamber with the plasma-cleaned glass slides. We also placed a Petri dish filled with the desiccant DrieRite™ in the vacuum chamber to further reduce ambient moisture. We allowed the reaction to proceed under vacuum overnight. The methyltrichlorosilane reacts with the silanol groups on the glass surface and covalently grafts methyl groups onto the glass thus rendering the surface hydrophobic[2].

Silanization of tracing paper: We perform solution phase silanization of pieces of tracing paper following previously reported protocols[3]. Working in a chemical fume hood, we prepared 10 mL

of a 80/20 by volume mixture of neat anhydrous toluene and neat methyltrichlorosilane in a clean glass vial. We placed 9 pieces of tracing paper 9.5 mm in diameter into the silane solution, capped the vial, and allowed the reaction to proceed for 30 minutes. We then removed the paper from the silane solution and washed the paper with excess neat toluene 5 times to remove unreacted silanes. We allowed the paper to dry in the fume hood for 30 minutes, and then transferred the paper to a 65 °C oven for 2 hours.

3. Characterization of the substrates

Scanning electron microscopy (SEM): SEM images of the dry substrates were obtained using a field emission scanning electron microscope (GeminiSEM 500, Zeiss, Germany). The substrates were cut into small 2 × 2 mm squares and mounted on aluminum stubs using double-sided copper tape. A piece of copper tape was placed on top of the substrate at one edge and was connected to the stub to create a conduction path to minimize charging at the surface. The beam accelerating voltage was set to 1 kV. We used an Everhart-Thornley secondary electron detector to collect the secondary electrons that scattered from the surface. Images were captured at a lateral pixel resolution of 1.09 μm/pixel [1120 μm × 840 μm (1024 pixels × 768 pixels)], and 21 nm/pixel [22.76 μm × 17.07 μm (1024 pixels x 768 pixels)].

Measurement of the average fiber diameter and length: Using ImageJ, we measure the diameters of 82 randomly selected nanocellulose fibers from SEM images of the paper. The average diameter of the fibers was 34 ± 11 nm. To determine the nanofibril length, we measure the end-to-end length of 47 fibers. The average length of the fibers was 5 ± 2 μm.

4. Quantification of the sizes and molar yields of the GUVs

Confocal microscopy of harvested vesicles: We constructed imaging chambers by covalently bonding custom-made PDMS gaskets with a square opening (width × length × height = 6 × 6 × 1 mm) to glass microscope slides. Before use, we passivated the chamber with a solution of 1 mg/mL casein to prevent rupture of the GUVs on the bare glass[4]. We filled the passivated chamber with 58 μL of a 100 mM solution of glucose and added a 2 μL aliquot of the suspension of harvested GUVs. We allowed the GUVs to sediment for 3 hours before imaging. We captured images using an upright confocal laser-scanning microscope (LSM 880, Axio Imager.Z2m, Zeiss, Germany). We excited the TopFluor® dye with a 488 nm argon laser and collected fluorescence using a 10× Plan-Apochromat objective with a numerical aperture of 0.45. We imaged the entire area of the chamber using an automated tile scan routine (64 images [850.19 μm × 850.19 μm (3212 pixels × 3212 pixels)]). The routine used an autofocus feature at each tile location. The pinhole was set at 12.66 Airy Units which gave a confocal slice thickness of 80 μm.

Image processing and data analysis: We analyzed the confocal tilescan images using a custom MATLAB routine[5] (Mathworks Inc., Natick, MA). The routine thresholded the images and then applied a watershed algorithm to segment the fluorescent objects from the background. We used the native *regionprops* function to obtain the equivalent diameters and mean intensities of the segmented objects. GUVs were selected from the detected objects based on the coefficient of variance of the intensities. GUVs fall within 1 – 2 times the full width at half the maximum (FWHM) of the highest peak in the coefficient of variance histogram. Once selected, we used MATLAB native routines to obtain the diameters and the counts of the GUVs. We plot size histograms, calculate the molar yields, and perform statistical tests.

Size distributions: We used MATLAB to plot histograms of the vesicle diameters for each repeat using 1 μm wide bins. The bins were normalized to show the GUV counts per μg of lipid deposited

(10 µg for all substrates). We take a mean of the counts in each bin from the histograms of the 5 independent repeats per surface to plot the results in Supplementary Fig. 2a-g.

Calculation of median diameters: We calculated the median diameter of the population from each of the 5 independent repeats using the native median command in MATLAB. We then take a mean of these 5 values to prepare the plot in Fig. 4b.

Calculation of extreme sizes: We calculated the average diameter of the 100 vesicles with the largest diameter in each distribution. We then take a mean of this value from the 5 independent repeats for Fig. 4c.

Calculation of molar yield: We obtain the moles of lipid in *N* GUVs from a harvested suspension using Equation (3.7.1).

$$mol_{GUV} = \frac{2\pi V_h}{N_A A_{hg} V_{al}} \sum_{i=1}^{N} (d_i)^2 \tag{3.7.1}$$

In this equation, N_A is Avagadro's number, A_{hg} is the lipid headgroup area, V_h is the volume of the harvested suspension, V_{al} is the volume of the aliquot, and d_i is the diameter of vesicle i. The factor of 2 accounts for the 2 lipid leaflets in a bilayer. The molar amount of GUVs of a given diameter can be obtained by summing GUVs of a specific diameter. In the main text, we defined three size ranges, small GUVs ($1 \leq d_i < 10$), large GUVs ($10 \leq d_i < 50$) and very large GUVs ($d_i \geq 50$).

$$mol_{GUV} = mol_{\text{small GUVs}} + mol_{\text{large GUVs}} + mol_{GUVs \geq 50} \tag{3.7.2}$$

$$mol_{GUV} = \frac{2\pi V_h}{N_A A_{hg} V_{al}} \left(\sum_{i=1}^{N_{d<10}} (d_i)^2 + \sum_{i=d\geq 10}^{N_{d<50}} (d_i)^2 + \sum_{i=d\geq 50}^{N} (d_i)^2 \right) \tag{3.7.3}$$

To obtain the molar yield, Y_{mol} we divide the mols of lipids in the GUV membranes with the total mols of lipid deposited on the substrate (kept the same for all substrates)and report the ratio as a percentage.

$$Y_{mol} = \frac{mol_{GUV}}{mol_{tot}} \times 100\% \quad (3.7.4)$$

Statistical Tests: We performed all statistical tests in MATLAB. For statistical testing, the groups were assigned by technique, group 1: gentle hydration on glass, group 2: gentle hydration on regenerated cellulose dialysis membranes, group 3: gentle hydration on nanopaper, group 4: gentle hydration on tracing paper, group 5: gentle hydration on silanized glass, group 6: gentle hydration on silanized tracing paper, group 7: electroformation. We test for statistical significance of differences in the mean molar yields by performing a balanced one-way Analysis of Variance (ANOVA) followed by a post-hoc Tukey's honestly significant test (HSD). An ANOVA assumes that the repeats drawn for each group comes from a normal distribution and that the variances between each group is equal. We conducted an Anderson Darling test to determine normality. The results of the test are shown in Supplementary Table 2. All repeats within a group were consistent with being drawn from a normal distribution. We conducted a Bartlett's test to determine if the variances of the groups were equal. Results of the tests are shown in Supplementary Table 2. The variances between groups were equal. Thus, the data satisfies the criteria for an ANOVA. We show the ANOVA table and post-hoc HSD tables in Supplementary Table 3. We also make summary conclusions in the table.

5. In situ imaging on the surface of the substrate

Imaging on the surface: We prepared the lipid-coated substates following the same standard procedures we used for quantification of the molar yield. Instead of using the 48-well plates for

growth, we used circular PDMS gaskets (inner diameter × height = 12 mm × 1 mm) affixed to glass slides. After hydrating with 150 μL of growth buffer, we sealed the chamber with a glass coverslip. We captured images after 2 hours of growth using a confocal microscope. We excited the TopFluor® dye with a 488 nm argon laser and imaged using a 10× Plan-Apochromat objective with a numerical aperture of 0.45.

6. Fluorescence recovery after photobleaching vesicle buds and isolated vesicles

Vesicle buds: Fluorescence recovery after photobleaching (FRAP) experiments were performed using a 488 nm argon laser. Circular regions of closely-packed vesicle buds (~40 μm in diameter) were bleached at 100 % laser power. Time lapse images of the subsequent recovery were collected at 1 second intervals for 250 seconds using 0.1 % of the laser power. The mean intensity of the region of interest was measured using ImageJ. The plots were normalized to the pre-bleach intensity which was set to 1.

Isolated vesicles: To obtain closely-packed isolated vesicles, we pooled vesicles from 3 tracing paper samples to obtain 450 μL of the vesicle solution. We centrifuged the vesicles at 10,000 × g for 3 minutes and remove the top 300 μL leaving behind a 150 μL solution of concentrated vesicles. A 30 μL aliquot of the concentrated vesicles was added to a PDMS chamber containing 30 μL of glucose, and the chamber was sealed with a glass coverslip. We allowed the vesicles to sediment for 5 hours before imaging. We performed FRAP experiments on the isolated vesicles using the same conditions as those used for the vesicle buds.

7. Time lapse images of vesicle buds

We used time-lapse imaging to capture the dynamics of the vesicle buds on the surface of the substrates. We excited the dye in the vesicles using a 488 nm argon laser and collected the

fluorescence using a 20× water-dipping Plan-Apochromat objective with a numerical aperture of 1.0. We captured images of the vesicle buds on the surface of the tracing paper at 5 second intervals 3 minutes after hydration. Typical images covered an area of approximately 200 μm × 200 μm and had a pixel resolution of 0.12 μm.

8. Scale up and calculation of cost

Scale up: To conduct scale-up experiments we used a Paasche airbrush and compressor to spray lipid onto whole sheets of tracing paper 9" × 12" in size. We used PVA-coated gloves when working with the chloroform and performed all experiments in a chemical fume hood. To coat the paper, we prepared 9.6 mL of 1 mg/mL DOPC:TFC (99.5:0.5 mol %) lipid mixture in chloroform to mimic the same lipid mass as the 48-well plate experiments. We used a 0.66 mm cap at the end airbrush, set the compressor pressure to 20 PSI, and brushed the lipid across the surface at a rate of approximately 1" per second. We placed the lipid-coated sheet under vacuum for 1 hour to allow residual solvent to evaporate, and then placed the sheet in a 9" × 13" Teflon coated baking pan. We hydrated the sheet in 100 mL of 100 mM solution of sucrose and allowed the GUVs to assemble for 1 hour. To harvest the GUVs, we pipette across the surface using a 1 mL plastic transfer pipette. We store the harvested GUVs in 50 mL Eppendorf tubes.

Calculation of cost: The total fixed material costs of fabricating GUVs include the cost of the substrate and the cost of the lipids. To obtain the substrate costs, we calculated the cost per unit area (mm^2) of each substrate using the lowest prices posted in July 2020 on the websites of large multinational suppliers of scientific materials (Supplementary Table 4). To determine the number of vesicles harvested from a given area of substrate, we normalized the size histograms by dividing the counts in each bin (bin widths of 1 μm) by the area (mm^2) of substrate that was used to grow

vesicles, which for all of the experiments was 70.88 mm^2. The counts per area for each bin was divided by the substrate cost per area to obtain the substrate cost per vesicle (Fig. 8a). Additionally, all methods require the use of solvent, buffers, and fluid receptacles. For electroformation, additional equipment such as a function generator and a source of electrical power is required for directing the formation of vesicles. We do not consider these additional costs in our calculations.

Cyclic reuse of tracing paper: After harvesting the vesicles we rinsed the paper under a flowing stream of ultrapure water for 30 seconds and then soaked the paper in 10 mL of ultrapure water for 30 minutes. We occasionally agitated the paper in the water by manually shaking the container. This procedure removes any water-soluble residual sugars from the prior cycle of growth. We then moved the tracing paper to a 65°C oven to dry for 1 hour. To remove any residual lipid, we soaked the tracing paper in 10 mL of neat chloroform for 30 minutes. We occasionally agitated the paper in the chloroform by manually shaking the container. We then carefully removed the tracing paper and placed it in a laboratory vacuum chamber for 1 hour to remove traces of chloroform. After drying, the standard procedures for growth were employed to start the next cycle of growth.

Supporting Figures

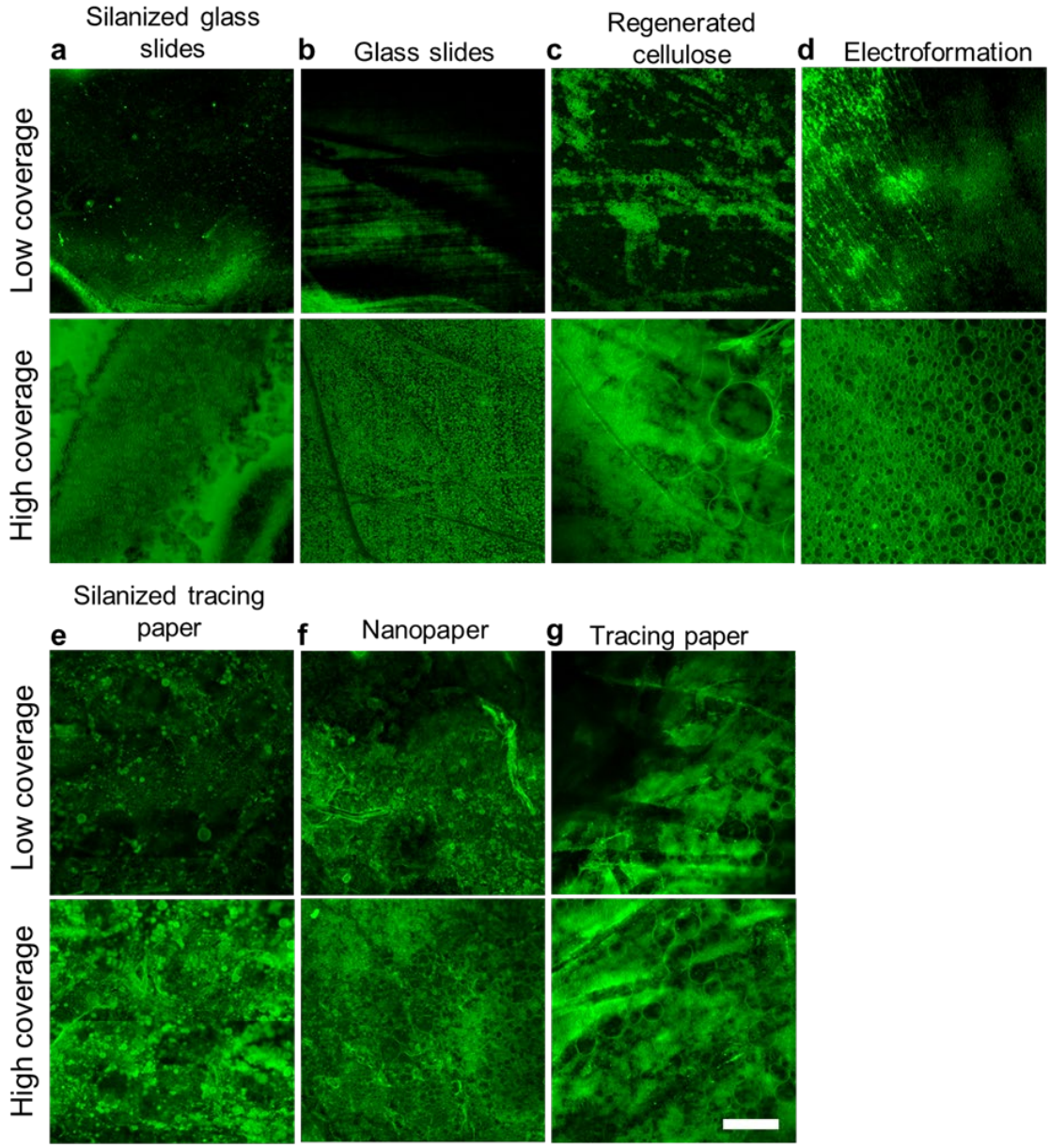

Figure S1. Characterization of the coverage of vesicle buds on the substrates. (a-d) Confocal images of regions with low and high vesicle bud coverage on (a) silanized glass slides, (b) glass slides, (c) regenerated cellulose and (d) electroformation. (e-g) Images of regions with low and high vesicle coverage on (e) silanized tracing paper, (f) nanopaper, and (g) tracing paper. Scale bar 100 μm.

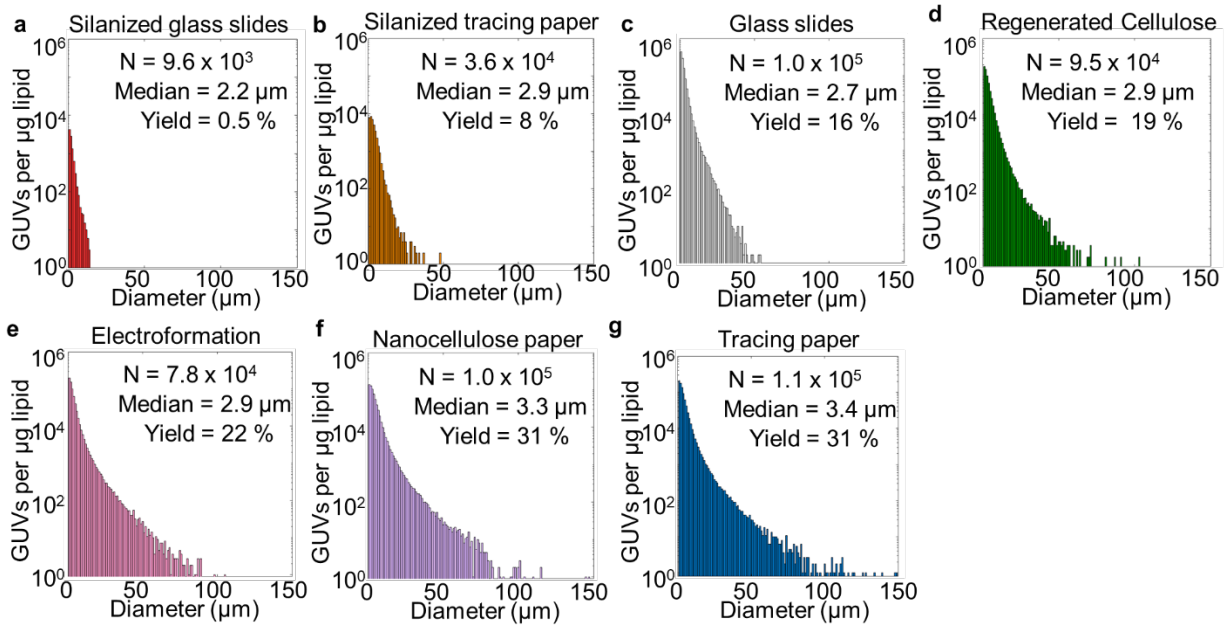

Figure S2. Histograms of GUV diameters that were obtained from the assorted substrates**.** Normalized histograms of the diameters of the GUVs harvested from (a) silanized glass slides, (b) silanized tracing paper, (c) glass slides, (d) regenerated cellulose dialysis membranes, (e) electroformation on ITO-covered glass slides, (f) nanocellulose paper, and (g) tracing paper. The number of GUVs counted, the median size, and the molar yield is added to each plot. Bin widths are 1 µm. Note the logarithmic scale on the *y*-axis.

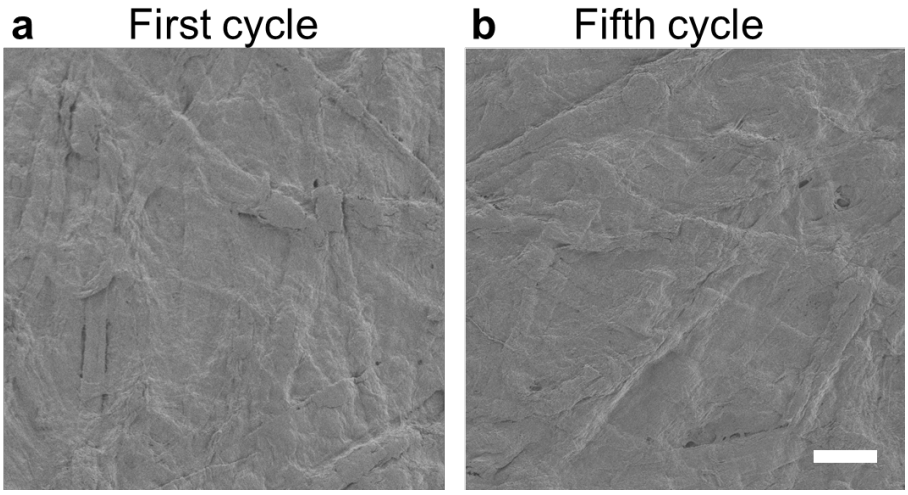

Figure S3. Characterization of the reused tracing paper surface. SEM images showing the surface structure of the tracing paper remains unchanged. (a) image after the first growth cycle and (b) image after the fifth growth cycle. Scale bar 50 μm.

Supplementary Tables

	Value	Electro.	Regen. Cellulose	Glass	Silanized Glass	Tracing Paper	Nanopaper	Silanzied Tracing Paper
Anderson Darling	p	0.5241	0.3831	0.847	0.4885	0.5251	0.3119	0.3739
Bartlett's Test	p	0.3462						

Table S1: Results of the Anderson-Darling and Bartlett tests. NS not significant, * $p < 0.05$, ** $p < 0.01$ *** $p < 0.001$.

Source	SS	df	MS	F	Prob > F, (p-value)
Columns	3725.24	6	620.873	90.53	5.0591E-17
Error	192.04	28	6.858		
Total	3917.27	34			

Group 1	Group 2	p-value	Significance	Comments
Glass	Electro-formation	0.00542	**	Effect of electric field significant
Glass	Regenerated Cellulose	0.383	NS	Effect of permeability not significant
Glass	Nanopaper	5.28E-08	***	Effect of curvature significant
Glass	Tracing Paper	4.31E-08	***	Effect of curvature significant
Glass	Silanized Glass	6.23E-08	***	Effect of hydrophilicity significant
Glass	Silanized TP	0.00304	**	Effect of hydrophilicity significant
Electro-formation	Nanopaper	5. 22E-04	***	Effect of curvature significant
Electro-formation	Tracing Paper	1.72E-04	***	Effect of curvature significant
Electro-formation	Regenerated Cellulose	0.439	NS	Effect of electric field not significant
Electro-formation	Silanized Glass	3.71E-08	***	Effect of hydrophilicity significant
Electro-formation	Silanized TP	1.14E-07	***	Effect of hydrophilicity significant
Tracing Paper	Nanopaper	0.999	NS	Effect of manufacturing paper not significant
Tracing Paper	Regenerated Cellulose	9.63E-07	***	Effect of curvature significant
Tracing Paper	Silanized Glass	3.71E-08	***	Effect of curvature significant
Tracing Paper	Silanized TP	3.71E-08	***	Effect of hydrophilicity significant
Nanopaper	Regenerated Cellulose	2.71E-06	***	Effect of curvature significant
Nanopaper	Silanized Glass	3.71E-08	***	Effect of curvature significant
Nanopaper	Silanzied TP	3.71E-08	***	Effect of hydrophilicity significant

Regenerated Cellulose	Silanized Glass	3.73E-08	***	Effect of hydrophilicity significant
Regenerated Cellulose	Silanized TP	1.18E-05	***	Effect of hydrophilicity significant
Silanized TP	Silanized Glass	0.00162	**	Effect of curvature significant

Table S2: ANOVA table and table of p-values from post hoc Tukey's HSD tests of the molar yields of GUVs obtained from gentle hydration on glass, regenerated cellulose, nanocellulose paper, tracing paper, silanized glass, and silanized tracing paper and from electroformation on ITO slides.

Parameter	Description	Magnitude	Source
κ_a	Area expansion modulus	$80 - 200 \times 10^{-3}$ J m^{-2}	[6]
ξ	Adhesion energy	-1×10^{-1} to -5×10^{-9} J m^{-2}	[6–8]
λ	Membrane edge energy	1×10^{-11} J m^{-1}	[6]
κ_B	Bending modulus	8.22 to 82.2×10^{-20} J	[6]
κ_G	Gaussian bending modulus	$-0.9\kappa_B$ to $-1.0\kappa_B$	[9]

Table S3: Values for the physical parameters of phosphocholine membranes reported in the literature.

Substrate	Cost (USD)	Unit of measure	Cost (USD) per mm^2	Source of cost
Glass Slide	733.61	1440 glass slides, 25 mm × 75 mm	2.72E-04	Fischer Scientific
ITO-slide	144	10 slides, 25 mm × 25 mm	2.30E-02	Sigma Aldrich
Regenerated Cellulose	224.5	1 roll, 30,000 mm × 90 mm	8.31E-05	Fischer Scientific
Tracing paper	26.93	500 sheets, 228.6 mm × 304.8 mm	7.73E-7	Amazon

Table S4: Material costs of substrates used to assemble GUVs. Costs per mm^2 were calculated using the most economical option available online at various large scientific supply companies.

Supporting References

(1) Herold, C.; Chwastek, G.; Schwille, P.; Petrov, E. P. Efficient Electroformation of Supergiant Unilamellar Vesicles Containing Cationic Lipids on ITO-coated Electrodes. *Langmuir* **2012**, *28*, 5518–5521.

(2) Glavan, A. C.; Martinez, R. V.; Subramaniam, A. B.; Yoon, H. J.; Nunes, R. M. D.; Lange, H.; Thuo, M. M.; Whitesides, G. M. Omniphobic "rF paper" Produced by Silanization of Paper with Fluoroalkyltrichlorosilanes. *Adv. Funct. Mater.* **2014**, *24*, 60–70.

(3) Yadav, A. R.; Sriram, R.; Carter, J. A.; Miller, B. L. Comparative Study of Solution-Phase and Vapor-phase Deposition of Aminosilanes on Silicon Dioxide Surfaces. *Mater. Sci. Eng. C* **2014**, *35*, 283–290.

(4) Faysal, K. M. R.; Park, J. S.; Nguyen, J.; Garcia, L.; Subramaniam, A. B. Lipid Bilayers are Long-lived on Solvent Cleaned Plasma-oxidized Poly(dimethyl) siloxane (ox-PDMS). *PLoS One* **2017**, *12*, 1–16.

(5) Pazzi, J.; Xu, M.; Subramaniam, A. B. A. B. Size Distributions and Yields of Giant Vesicles Assembled on Cellulose Papers and Cotton Fabric. *Langmuir* **2018**, *35*, 7798–7804.

(6) Israelachvili, J. N. *Intermolecular and Surface Forces*, 3rd ed.; Academic Press: Waltham, MA, 2011.

(7) Sun, Y.; Lee, C.; Huang, H. W. Adhesion and Merging of Lipid Bilayers : A Method for Measuring the Free Energy of Adhesion and Hemifusion. *Biophysj* **2011**, *100*, 987–995.

(8) Servuss, R. M.; Helfrich, W. Mutual Adhesion of Lecithin Membranes at Ultralow Tensions. *J. Phys.* **1989**, *50*, 809–827.

(9) Dharmavaram, S.; She, S. B.; Lázaro, G.; Hagan, M. F.; Bruinsma, R. Gaussian Curvature and the Budding Kinetics of Enveloped Viruses. *PLoS Comput. Biol.* **2019**, *15*, 1–22.